Enhancement and segmentation of breast thermograms

Trongtirakul, Thaweesak, Oulefki, Adel, Agaian, Sos, Chiracharit, Werapon

Thaweesak Trongtirakul, Adel Oulefki, Sos Agaian, Werapon Chiracharit, "Enhancement and segmentation of breast thermograms," Proc. SPIE 11399, Mobile Multimedia/Image Processing, Security, and Applications 2020, 113990F (21 April 2020); doi: 10.1117/12.2554594

SPIE.

Event: SPIE Defense + Commercial Sensing, 2020, Online Only, California, United States

Enhancement and Segmentation of Breast Thermograms

Thaweesak TRONGTIRAKUL[a], Adel OULEFKI[b], Sos AGAIAN[c], and Werapon CHIRACHARIT[d]

[a]Faculty of Industrial Education Rajamangala University of Technology Phra Nakhon, 399 Samsen Rd. Vachira Phayaban Dusit Bangkok 10300, Thailand
[b]Centre de Développement des Technologies Avancées — CDTA, PO. Box 17 Baba Hassen, Algiers 16081, Algeria
[c]Dept. of Computer Science, College of Staten Island, New York, 2800 Victory Blvd Staten Island, New York 10314, USA
[d]King Mongkut's University of Technology Thonburi, 126 Pracha Uthit Rd., Bang Mod, Thung Khru, Bangkok 10140, Thailand

ABSTRACT

Enhancement and segmentation of suspicious regions of a thermal breast image are among the most significant challenges facing radiologists while examining and interpreting the thermogram images. The proposed focuses to following problems: How can increase the contrast between cancer regions and the background, how to adjust the intensity of the presence of BC region to be more homogeneous in the infrared image; how to efficiently segment tumors as suspicious regions with a very weak contrast to their background and how to extract the relevant features which separate tumors from background. The proposed cancer segmentation scheme composed of three main stages: (i) image enhancement; (ii) detection of the tumor region; (iii) features extraction from the segmented tumor area followed by coloring the segmented region. The performance of the proposed enhancement and segmentation method was evaluated on DMR-IR database and the average segmentation Accuracy, MCC, Dice and Jaccard obtained are **98.8%**, **47.96%**, **43.03%**, and **34.8%** respectively which is better than FCM, LCV-LSM, and EM-GMM methods. Besides, we also investigate the role of thermal image enhancement in tumor characterization and feature extraction.

Keywords: Thermography images, Abnormality detection, Breast cancer (BC), Image enhancement, Image segmentation

1. INTRODUCTION

Breast cancer (BC) becomes more and more common nowadays since it is the second leading cause of death for women all over the world.[1] To address this women's specific concerns, an early diagnosis of BC is highly recommended. According to recent pathological studies, women whose diagnosed with the BC at an early stage have more than 90% of survival rate if treated in the first five years.[2] Thus,

Further author information: (Send correspondence to A.O or S.A)
A.O: E-mail: adel.oulefki@fulbrightmail.org, Telephone: +1 (917) 518-8425
S.A: E-mail: sos.agaian@csi.cuny.edu, Telephone: +1 (718) 982-2843

Mobile Multimedia/Image Processing, Security, and Applications 2020, edited by Sos S. Agaian, Vijayan K. Asari, Stephen P. DelMarco, Proc. of SPIE Vol. 11399, 113990F · © 2020 SPIE
CCC code: 0277-786X/20/$21 · doi: 10.1117/12.2554594

latterly many extensive research and studies have been carried out for detecting the BC on his early appearance. Scientists notice first that the blood vessels started to be created around cancerous cells area, it can cause increasing fluid propagation followed by producing heat spots leading to an increase of local temperature near the skin around cancerous tissue.[3] For the screening part, several sensors can be used for breast visualization,[4] including mammography,[5] IR,[6] MRI,[7] CT,[8] ultrasound,[7] and thermography scans.[9] Latterly, ultrasound and mammography were the most used sensors for the early localization of cancer. The mammography can be aggressive because of the electromagnetic radiations are considered as a stimulating factor for cancer development.[10] Furthermore, it is considered inconvenient. Ultrasound, on the other hand considered as effective for detecting the breast masses but suffers from a high degree of fault detection.[9] On the flip side, Infrared thermography (IRT) is a fast, non-contact, passive, and non-invasive procedure used to record and monitor body temperature remotely, or to provide information about subtle temperature changes in it. It is natural because it has long been recognized that body temperature is a sign of health or illness. Also, the skin temperatures of the breast tumor or a malignant melanoma are found to be several degrees higher than that of the surrounding area. As a result, the abnormal temperature at the skin surface can be used (1) to predict the location, size, and feature vectors of the tumor region, (2) to study the tumor evolution after a treatment procedure, (3) to diagnosis of breast cancer, skin cancer, diabetes neuropathy, and peripheral vascular disorders. With the advent of modern infrared cameras, data acquisition, and processing techniques, it is now possible to have real-time high-resolution thermographic images, which is likely to surge further research in this field. Therefore, current thermal images have low signal to noise ratio, blurry, he quality of the thermography images is poor, and low contrast are the significant limitations for segmentation, image analysis, and interpretation of medical thermal images which made the difficulty in evaluating the feasibility of using thermal imaging as a potential tool for detecting breast cancer.

The main aim of this paper is to develop thermography images based a combine tumor enhancement and segmentation algorithm, including (i) Increase the contrast between cancer regions and the background, (ii) Adjustment the intensity of the presence of BC region to be more homogeneous in the infrared image, (iii) Segment tumors as suspicious regions with a very weak contrast to their background, (iv) Extraction of relevant features in such a way to separate tumors from background. Finally, this paper is organized as follows. After briefly reviewing the related works on BC enhancement and segmentation in Section 2. Section 3 will describe the proposed framework and measurement analyses both on statistically and visually aspect (in Section 4) and in terms of the coloring of a segmentation algorithm (in Section 4 also). We conclude arguing (in Section 5) that proposed to achieve better results both on the subjective and objective aspects

2. RELATED WORKS

Generally, BC was a form of cancer disease that occurred in the breast tissues. These were obtained via obesity, family history and, reproduction factors. Nowadays, there was a majority of women that tackled the BC disease. The detection of breast tumor grade generally spotted based on certain warning signs such alterations in size, sustain pain, mutation of genes, redness on breast skin and skin texture.[11] In the current research section, the machine vision methods were assigned for the detection and classification of BC. It was utilized to give high accuracy and effective treatment capabilities.

Authors proposed several theories proposed to detect the early stage of BC, some focusing on segmentation and enhancement, others on classification. Generally, there are five databases namely

MIAS,[12] INbreast[13] , NYU SofM , DDSM,[14] DMR-IR,[15] while most authors use thermogram or mammography sensing approaches for the detection.

In terms of enhancement there are a large number of published methods, in (e.g., Oulefki et al. 2018 Iratni et al. 2018 ;[16],[1718]) authors involved image processing stage to enhance images captured in low-light conditions. Furthermore, improvement strategies might include frequency[1920] and spatial domain[2122] to improve images. For instance, Du et al.[19] introduced (DWT) discrete wavelets transform in which they applied (HE) Histogram Equalizer to low frequency along with accentuating the high frequency coefficients. In[23] Jobson et al. (1997) presented (MSR) multiscale retinex approach which is the (HE) extension of the previous single-scale center/surround retinex. Due to its fast implementation.[24] HE considered as one of the basic method for enhancing and improving the contrast of images. In spite of its accuracy, it remains an uneven particularly when it processed under varying lighting conditions. Pizer et al.[2526] (CLAHE) summarized Contrast-Limited Adaptive Histogram Equalization. CLAHE computes distinct histograms blocks corresponding to a divided section of the input image then readjust the image's brightness of each part. But, CLAHE has a tendency to over-enhance images which led to loss of information in some local region.

On the flip side, accurate segmentation is unavoidable for radio-graphic interpretation[27] which consists of significantly extract image features from medical images with the aim to identify non-invasive image-based substitute for diagnosis and for predicting treatment feedback. In the literature several approaches have been developed for segmenting the BC or Region Of Interest (ROI). Kegelmeyer et al. in[28] introduced binary decision tree classifier and laws textural feature to classify between normal and lesions tissues. In[29] initiate SVM classifier for mass detection. In[30] authors proposed an CAD system fully automatic for mass detection based on (GLCM) gray level co-occurrences matrices. While Sahiner et al.[31] applied (GLDS) four gray-level difference statistics texture features and convolution neural network for mass detection. Dominguez et al.[32] suggested density slicing technique for tumor segmentation. Kashyap et al.[33] proposed an efficient segmentation approach for BC detection in mammograms images. Despite the fact that in the literature there seem to be several image segmentation techniques. But as yet there is still no particular approach that can be applied to any type of medical images. Algorithm development for one application of image segmentation may not always be applied to other class of images.

Toward the end of improving both segmentation and enhancement of BC for thermal images, we propose in this paper a hybrid segmentation-enhancement pipeline. Firstly, The proposed method consists of the stage of enhancement to increase the homogeneity regions of a giving thermal image, followed by segmentation stage. The details of the proposed methods are presented in the next section.

3. PROPOSED FRAMEWORK

Thermography becomes best from other sensing approaches for the better diagnose of the disease by screening.[34] The work was all about the enhancement and segmentation of BC in such a way to give to the radiologists the preliminary analysis and interpretation to better understand the type of images to detect the disease by using image processing approaches. Basically, digital image processing becomes an interesting area of research almost in every field[353637] and had a lot of attention in the medical field for its vast range of application of detection diseases. Image segmentation process was an approach to detect and screening of images of diseases such as cancer disease. The image segmentation was described in detail in this work and it included enhancement method.

The first step in the process of BC localisation is to enhance the input thermal image. This stage aims to suppress noise meanwhile increase contrast of a giving image In the literature there are many

enhancement approaches[36383940414 2 .43] But, these approaches are not suitable for medical images and can also produce significant noise. The main aim of luminance adjustion function is to increase the details by changing intensity values. However, the luminance of hot spot (cancer region) are close to other (background or non-cancer) region. To increase the differentiation between regions, we applied the approach named adaptive weighting metric to enhance two features (cancer and non cancer region). The mathematical details on the proposed enhancement and segmentation algorithm are summarized on Algorithm 1 and Algorithm 2 respectively. Firstly, image enhancement of the input image is applied simultaneously on the entire image and the segmented region ROI. Thereafter, the block-based identification is applied to the region-colored transparency and region classification. This last provides a masking metric. On the other hand, the former provides transparent color layers to fill the fusing featured image with the color. Finally, this resulting image is compared with the input image to obtain the selected colored breast segment. Final stage is recoloring in such a way to help radiologists to visualize accurately the abnormalities. All the steps applied to segment the BC are described on the below Figure 1.

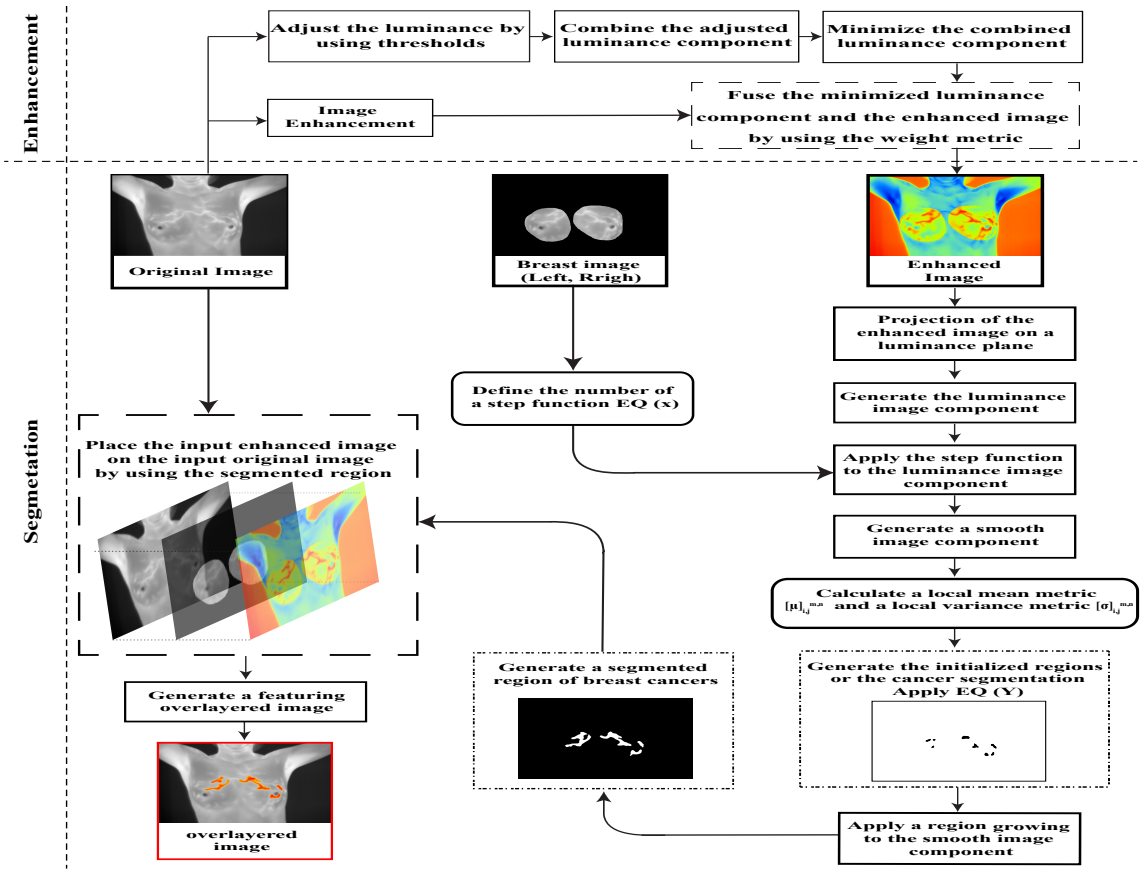

Figure 1: Flowchart of the proposed thermal enhancement and segmentation of breast cancer

Algorithm 1 Enhancement

Input: $I = \{I_{i,j}\}$ intensity of the image at the spatial address i, j and $I \in \{I_0, I_1, ..., I_L - 1\}$

// Where L discrete luminance levels denoted as $I = \{I_0, I_1, ..., I_L - 1\}$

1 Derivative Gaussian Filter

$$[I_B]_{i,j} = [I_B]_{i,j} \bigotimes K_{m,n}; K_{m,n} = G_{m,n} \cdot K_{m,n} \tag{1}$$

// $G = \{G_{m,n}\}$ and $M = \{M_{m,n}\}$ represent the Gaussian image filter and the mean filter, where $\sum_{m,n=-\infty}^{m,n=+\infty}$, $M_{m,n} = 1$ and $G_{i,j}$ and $M_{m,n}$ denote the weight of the filters at the local spatial location m, n.

// Where $[I_g]_{i,j}$ is ther first ordered gaussian image, which can be calculated as $[I_g]_{i,j} = I_{i,j} \bigotimes G_{m,n}$. $\bigotimes$ represents a convolution operator.

2 ROI localisation by applying (Soft Masking Metric)[44]

$$[I_{GM}]_{i,j} = [I_B]_{i,j} \cdot SM_{i,j} \tag{2}$$

$$SM_{i,j} = \begin{cases} 1, [I_g]_{i,j} \geq [I_B]_{i,j} \\ ([I_g]_{i,j}/[I_B]_{i,j})^r, [I_g]_{i,j} < [I_B]_{i,j} \end{cases} \tag{3}$$

// Where r is a gamma correction parameter

3 Calculation of Mean Threshold

- Mean region threshold: $t_m = \frac{\frac{1}{P \cdot Q} \sum_{p=1}^{P} \sum_{q=1}^{Q} R_{p,q}}{max\{R_{p,q}\}}$
- Variance region threshold: $t_v = max\left\{\omega_b \sigma_b^2 + \omega_f \sigma_f^2\right\}$
- Logarithmic-mean region threshold: $t_{lm} = \left| log^{\gamma} \left(\frac{\frac{1}{P \cdot Q} \sum_{p=1}^{P} \sum_{q=1}^{Q} R_{p,q}}{max\{R_{p,q}\}} \right) \right|$
- Logarithmic-variance region threshold:$t_{lv} = log^{\gamma} |(max\left\{\omega_b \sigma_b^2 + \omega_f \sigma_f^2\right\})|$

// Where P and Q are the region of interest size. $\omega_{(.)}$ represent a weight of a background region $(.)_b$ and a foreground region $(.)_f$, b and f are L discret luminance level. γ is a logarithmic power factor.

4 Luminance adjustment

$$LA_{i,j} = \begin{cases} \frac{e^{-(\frac{(x_{i,j} - t_{(.)})^2}{\delta})} - e^{-(\frac{(t_{(.)})^2}{\delta})}}{-(\frac{(t_{(.)})^2}{\delta})}, 0 \leqslant x_{i,j} < t_{(.)} \\ \frac{e^{-(\frac{(x_{i,j} - t_{(.)})^2}{\delta})} - e^{-(\frac{(t_{(.)})^2}{\delta})}}{1 - e^{-(\frac{(t_{(.)})^2}{\delta})}}, t_{(.)} \leqslant x_{i,j} \leqslant 1 \end{cases} \tag{4}$$

// $x_{i,j} = \frac{[I_{GM}]_{i,j}}{max[I_{GM}]_{i,j}}$ denote a normalized soft-masked image, which $x_{i,j} \leqslant 1$.

/* Fusion */

5 Image fusion

$$F_{i,j} = \omega_{i,j} \cdot min_k \{LA_{i,j,k}\} + (1 - \omega_{i,j}) \cdot Y_{i,j} \tag{5}$$

// Where k is the number of luminance adjustment image components, which composed of three-dimensional direction. $Y_{i,j}$ denotes an enhanced image and $\omega_{i,j}$ is a weighting metric, $\omega_{i,j} = \frac{1}{L-1} min_k \{LA_{i,j,k}\}$

Output: Enhanced image

Algorithm 2 Segmentation

Input: Enhanced Image

6 Step unit classification

$$\begin{cases} 0, l < \frac{\rho(L-1))}{C}; \rho = 1 \\ 1, l < \frac{\rho(L-1))}{C}; \rho = 2 \\ \vdots \\ C, l < \frac{\rho(L-1))}{C}; \rho = n \end{cases} \tag{6}$$

// Where n represents the number of luminance classes

7 Region growing initialization and region growing segmentation

$$J_{i,j} = \begin{cases} 0, \delta_l(X_{i,j}) < [\mu]_{i,j}^{m,n} + \alpha \\ 1, \delta_l(X_{i,j}) > [\mu]_{i,j}^{m,n} + \alpha \end{cases} \tag{7}$$

// $X_{i,j}$ denote a luminance component, consisted of l discrete levels. $[\mu]_{i,j}^{m,n}$ represents a local mean metric generated by the local block size $m - by - n$. α is constant. To initialize the beginning regions of cancer segmentation

/* Overlay features */

8 Feature overlaying

$$O_(i,j,k) = \begin{cases} I_{i,j,k}, S_{i,j} = 0 \\ T_{i,j,k}, S_{i,j} = 1 \end{cases} \tag{8}$$

// $S_(i,j)$ denote the segmented image, located into the permitted range $[0,1]$. $I_(i,j,k)$ and $T_(i,j,k)$ represent an original thermal breast cancer image and the enhanced-recoloring image, respectively

Output: Segmented image

Data: Testing on 10 images from DMR database[45]

4. RESULTS AND DISCUSSIONS

In order to evaluate the performance of the proposed segmentation approach, the statistical values of the breast thermograms segmentation are compared with the result of the FCM,[46] LCV-LSM[47] and EM-GMM.[48] Thermograms of the patients with breast tumors that are considered as abnormal thermograms by a medical expert.[49] On the other hand, when there is no sign of cancer the patients are considered normal and healthy thus no segmentation are required. There is an extensive literature to evaluate the performance of the proposed using segmentation quality metrics. In our case, we pick: Accuracy,[50] MCC (Mathew Correlation Coefficient),[50] Dice,[51] Jaccard[50] to evaluate statistically the performance of the proposed against the well-known algorithm used in cancer segmentation FCM, LCV-LSM, and EM-GMM. A higher value obtained from the aforementioned metrics implies a better segmentation performance. The exact mathematical details of the Accuracy, FMeasure, MCC (Mathew Correlation Coefficient), Dice, and Jaccard can be found in the giving reference,[50].[51]

4.1 Quantitative comparison

For statistical analysis, the mean of ACC, MCC, Dice, and Jaccard are computed from both left, and right breasts. Then, the mean values of left and right breasts together are also computed for all breast thermograms to show the efficiency of segmentation in breast abnormality detection. From the mean

values listed in Table 1, it has been seen that the average of all the four metrics: ACC, MCC, Dice, and Jaccard are significantly higher using the proposed than the average of the FMC, LCV-LSM and EM-GMM approaches, where the last approach compete in term of ACC, Dice, and Jaccard meterics at the right side of the breast only.

Table 1: Mean values of evaluation of the proposed against FCM, LCV-LSM, and EM-GMM using ACC, MCC, Dice, and Jaccard segmentation metrics

	Metric											
Method	ACC			MCC			Dice			Jaccard		
	Left	Right	Both	Left	Right	Both	Left	Right	Both	Left	Right	Both
Proposed	0.991	0.991	0.982	0.466	0.469	0.504	0.460	0.327	0.499	0.319	0.221	0.339
FCM	0.985	0.979	0.964	0.398	0.360	0.344	0.399	0.186	0.305	0.286	0.123	0.201
LCV-LSM	0.896	0.927	0.872	0.009	0.027	0.126	0.026	0.099	0.138	0.013	0.025	0.076
EM-GMM	0.935	0.994	0.952	0.422	0.438	0.387	0.368	0.432	0.361	0.229	0.275	0.229

The results are also expressed by using box-plots in Figure 3 by using colors blue for proposed, red for FCM, brown for LCV-LSM, and black for EM-GMM. Each vertical axis shows Accuracy, MMC, Dice, and Jaccard metrics and the horizontal axis shows the proposed, FCM, LCV-LSM, and EM-GMM for evaluating the performance of the segmentation of each approach. Box-plot also can show the median. On each box, the vertical line denotes the median, the vertical lines outside each box identify the upper and lower whiskers. As can be seen in Figure 3 and since higher overall values obtained from Accuracy, MMC, Dice, and Jaccard metrics implies a better segmentation performance. It is obvious from the summary statistics of the aforementioned metrics that the results provided by the proposed segmentation is greater than other approaches picked for comparison.

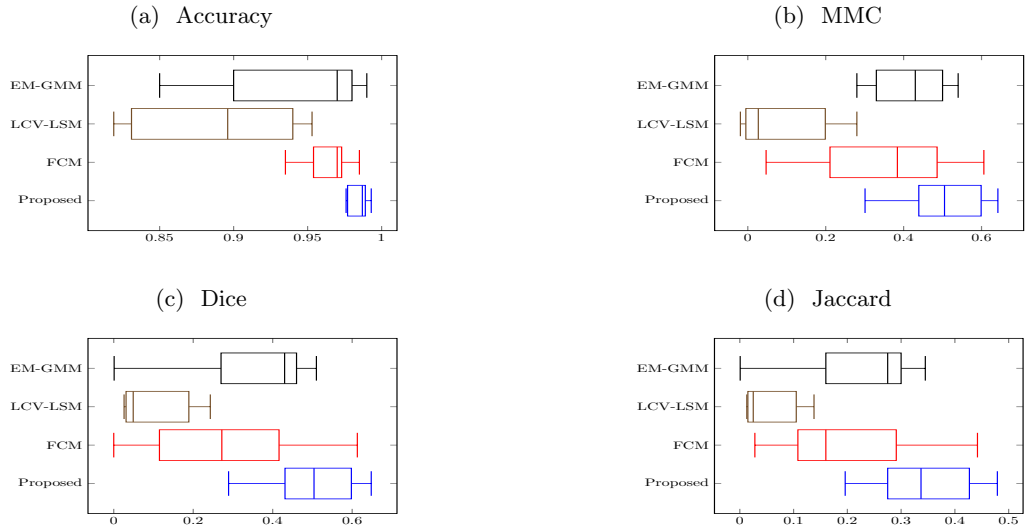

Figure 2: Box-plot of median values of the proposed against FCM, LCV-LSM, and EM-GMM segmentation approaches using ACC, MCC, Dice, and Jaccard metrics

4.2 Qualitative comparison

In Tab. 2, we qualitatively compared visually our segmentation results with the ground-truths, against three state-of-the-art BC segmentation approaches FCM, LCV-LSM, and EM-GMM. The first and second columns show the original images from the DMR-IR database and corresponding ground truth segmentation results. The third and fourth columns illustrate the segmentation results of FCM, LCV-LSM, and EM-GMM respectively. Fifth and sixth columns illustrate the segmentation results of the proposed along with its overlying.

By comparing the visual segmentation results of proposed with the ground truth images, it can be observed that the tumor segmentation is almost in exact shape. In contrast, both FCM and LCV-LSM misses some of the breast areas or over-segmentation such us in first and the last rows. Besides, for the images in the second raw, FCM, segmented the breast region along with a significant amount of non-tumor on the right side of the body. Whereas, the proposed precisely segments the cancer region. It must be noted that the FCM, LCV-LSM, and EM-GMM have produced over-segmentation results for all the images in Tab. 2 though the proposed has produced consistent segmentation results.

Original	GT	FCM	LCV-LSM	EM-GMM	Proposed	Overlaying

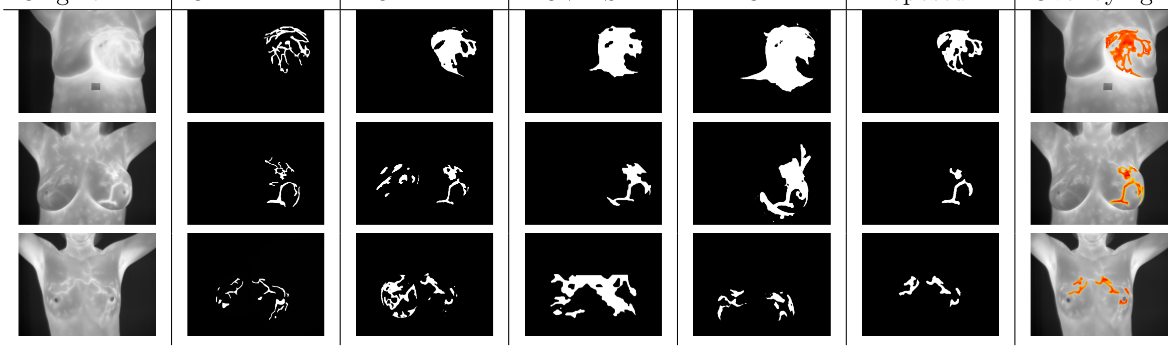

Table 2: Breast cancer comparison. Column 1: Original thermal images having breast cancer, column 2: Ground Truth, column 3: segmentation using FCM, column 4: segmentation using LCV-LSM, column 5: segmentation using EM-GMM, column 6: segmentation using proposed, column 7: Overlaying using proposed

From the above discussion, it can be concluded that the proposed BC segmentation has the potential to produce satisfactory results, even when input images images are blurred and boundaries are indistinct as shown in the images in Fig. 3.

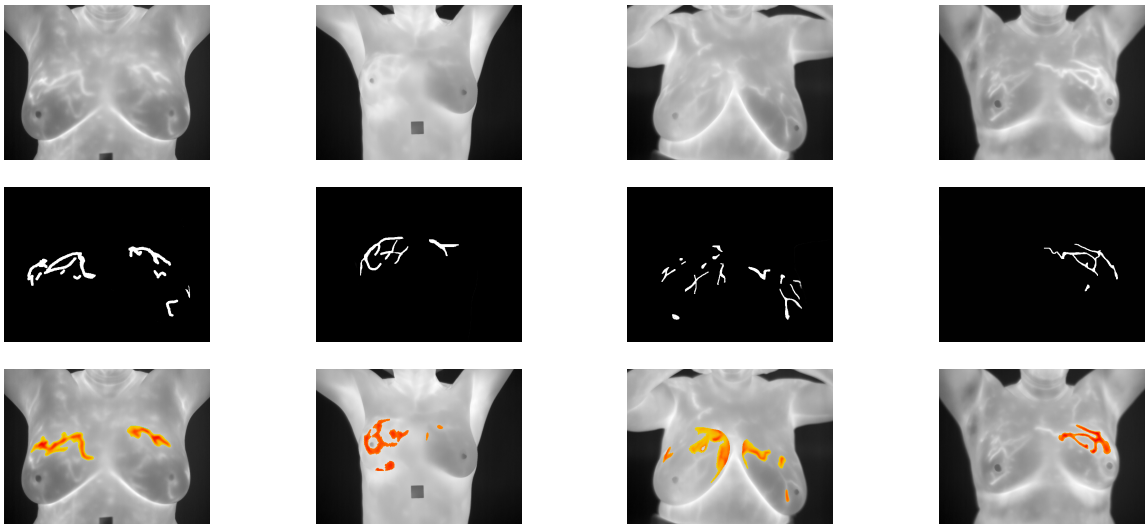

Figure 3: Samples of breast cancer overlaying using proposed; first raw original images, second raw the ground truth of the corresponding images, third raw overlaying images after segmentation

5. CONCLUSION

The accurate enhancement and segmentation of suspicious breast tumor structure is a crucial step to support the medical professional (radiologist) in the interpretation of the BC. The proposed framework could assist the medical professional to evaluate in real-time the appearance of a possible BC. The proposed first attempts to enhance the thermograph images and then segment the tumor by extracting and coloring the (ROIs) containing the BC. The texture features of BC are extracted and the segmentation performance is calculated using Accuracy, MCC, Dice and Jaccard metrics. The proposed system uses the images from the DMR-IR database of both left and the right then both breast breasts together. The overall segmentation performance of the proposed method are **98.8%**, **47.96%**, **43.03%**, and **34.8%** respectively when measured using Accuracy, MCC, Dice, and Jaccard index. Even-though the proposed approach has shown good results in terms of overall accuracy, MCC, Dice, and Jaccard. But more emphasis can be given to the classification stage in the future.

REFERENCES

[1] Cheng, H.-D., Shan, J., Ju, W., Guo, Y., and Zhang, L., "Automated breast cancer detection and classification using ultrasound images: A survey," *Pattern recognition* **43**(1), 299–317 (2010).

[2] Galea, M. H., Blamey, R. W., Elston, C. E., and Ellis, I. O., "The nottingham prognostic index in primary breast cancer," *Breast cancer research and treatment* **22**(3), 207–219 (1992).

[3] Fox, S. B., Gatter, K. C., Leek, R. D., Harris, A. L., Bliss, J., Mansi, J. L., and Gusterson, B., "Association of tumor angiogenesis with bone marrow micrometastases in breast cancer patients," *Journal of the National Cancer Institute* **89**(14), 1044–1049 (1997).

[4] Wang, L., "Microwave sensors for breast cancer detection," *Sensors* **18**(2), 655 (2018).

[5] Cheng, H.-D., Shi, X., Min, R., Hu, L., Cai, X., and Du, H., "Approaches for automated detection and classification of masses in mammograms," *Pattern recognition* **39**(4), 646–668 (2006).

[6] Keyserlingk, J., Ahlgren, P., Yu, E., and Belliveau, N., "Infrared imaging of the breast: Initial reappraisal using high-resolution digital technology in 100 successive cases of stage i and ii breast cancer," *The Breast Journal* **4**(4), 245–251 (1998).

[7] Lee, C. H., Dershaw, D. D., Kopans, D., Evans, P., Monsees, B., Monticciolo, D., Brenner, R. J., Bassett, L., Berg, W., Feig, S., et al., "Breast cancer screening with imaging: recommendations from the society of breast imaging and the acr on the use of mammography, breast mri, breast ultrasound, and other technologies for the detection of clinically occult breast cancer," *Journal of the American college of radiology* **7**(1), 18–27 (2010).

[8] Rosen, E. L., Eubank, W. B., and Mankoff, D. A., "Fdg pet, pet/ct, and breast cancer imaging," *Radiographics* **27**(suppl_1), S215–S229 (2007).

[9] Arena, F., Barone, C., and DiCicco, T., "Use of digital infrared imaging in enhanced breast cancer detection and monitoring of the clinical response to treatment," in [*Proceedings of the 25th Annual International Conference of the IEEE Engineering in Medicine and Biology Society (IEEE Cat. No. 03CH37439)*], **2**, 1129–1132, IEEE (2003).

[10] Jesneck, J. L., Lo, J. Y., and Baker, J. A., "Breast mass lesions: computer-aided diagnosis models with mammographic and sonographic descriptors," *Radiology* **244**(2), 390–398 (2007).

[11] Harbeck, N. and Gnant, M., "Breast cancer," *The Lancet* **389**, 1134–1150 (2017).

[12] Suckling, J., Parker, J., Dance, D., Astley, S., Hutt, I., Boggis, C., Ricketts, I., Stamatakis, E., Cerneaz, N., Kok, S., et al., "Mammographic image analysis society (mias) database v1. 21," (2015).

[13] Moreira, I. C., Amaral, I., Domingues, I., Cardoso, A., Cardoso, M. J., and Cardoso, J. S., "Inbreast: toward a full-field digital mammographic database," *Academic radiology* **19**(2), 236–248 (2012).

[14] Lee, R. S., Gimenez, F., Hoogi, A., Miyake, K. K., Gorovoy, M., and Rubin, D. L., "A curated mammography data set for use in computer-aided detection and diagnosis research," *Scientific data* **4**, 170177 (2017).

[15] Santana, M. A. d., Pereira, J. M. S., Silva, F. L. d., Lima, N. M. d., Sousa, F. N. d., Arruda, G. M. S. d., Lima, R. d. C. F. d., Silva, W. W. A. d., and Santos, W. P. d., "Breast cancer diagnosis based on mammary thermography and extreme learning machines," *Research on Biomedical Engineering* (AHEAD), 0–0 (2018).

[16] Iratni, A., Aouache, M., and Adel, O., "Adaptive gamma correction-based expert system for nonuniform illumination face enhancement," *Journal of Electronic Imaging* **27**(2), 023028 (2018).

[17] Oulefki, A., Mustapha, A., Boutellaa, E., Bengherabi, M., and Tifarine, A. A., "Fuzzy reasoning model to improve face illumination invariance," *Signal, Image and Video Processing* **12**(3), 421–428 (2018).

[18] Mustapha, A., Oulefki, A., Bengherabi, M., Boutellaa, E., and Algaet, M. A., "Towards nonuniform illumination face enhancement via adaptive contrast stretching," *Multimedia Tools and Applications* **76**(21), 21961–21999 (2017).

[19] Du, S. and Ward, R., "Wavelet-based illumination normalization for face recognition," in [*Image Processing, 2005. ICIP 2005. IEEE International Conference on*], **2**, II–954, IEEE (2005).

[20] Hu, H., "Illumination invariant face recognition based on dual-tree complex wavelet transform," *IET Computer Vision* **9**(2), 163–173 (2014).

[21] Sheet, D., Garud, H., Suveer, A., Mahadevappa, M., and Chatterjee, J., "Brightness preserving dynamic fuzzy histogram equalization," *IEEE Transactions on Consumer Electronics* **56**(4) (2010).

[22] Poddar, S., Tewary, S., Sharma, D., Karar, V., Ghosh, A., and Pal, S. K., "Non-parametric modified histogram equalisation for contrast enhancement," *IET Image Processing* **7**(7), 641–652 (2013).

[23] Jobson, D. J., Rahman, Z.-u., and Woodell, G. A., "A multiscale retinex for bridging the gap between color images and the human observation of scenes," *IEEE Transactions on Image processing* **6**(7), 965–976 (1997).

[24] Wang, Y., Chen, Q., and Zhang, B., "Image enhancement based on equal area dualistic sub-image histogram equalization method," *IEEE Transactions on Consumer Electronics* **45**, 68–75 (Feb 1999).

[25] Pizer, S. M., "Contrast-limited adaptive histogram equalization: Speed and effectiveness stephen m. pizer, r. eugene johnston, james p. ericksen, bonnie c. yankaskas, keith e. muller medical image display research group," in [*Proceedings of the First Conference on Visualization in Biomedical Computing, Atlanta, Georgia, May 22-25, 1990*], 337, IEEE Computer Society Press (1990).

[26] Lu, L., Zhou, Y., Panetta, K., and Agaian, S., "Comparative study of histogram equalization algorithms for image enhancement," in [*Mobile Multimedia/Image Processing, Security, and Applications 2010*], **7708**, 770811, International Society for Optics and Photonics (2010).

[27] Kumar, V., Gu, Y., Basu, S., Berglund, A., Eschrich, S. A., Schabath, M. B., Forster, K., Aerts, H. J., Dekker, A., Fenstermacher, D., et al., "Radiomics: the process and the challenges," *Magnetic resonance imaging* **30**(9), 1234–1248 (2012).

[28] Kegelmeyer Jr, W. P., Pruneda, J. M., Bourland, P. D., Hillis, A., Riggs, M. W., and Nipper, M. L., "Computer-aided mammographic screening for spiculated lesions.," *Radiology* **191**(2), 331–337 (1994).

[29] Campanini, R., Dongiovanni, D., Iampieri, E., Lanconelli, N., Masotti, M., Palermo, G., Riccardi, A., and Roffilli, M., "A novel featureless approach to mass detection in digital mammograms based on support vector machines," *Physics in Medicine & Biology* **49**(6), 961 (2004).

[30] Bellotti, R., De Carlo, F., Tangaro, S., Gargano, G., Maggipinto, G., Castellano, M., Massafra, R., Cascio, D., Fauci, F., Magro, R., et al., "A completely automated cad system for mass detection in a large mammographic database," *Medical physics* **33**(8), 3066–3075 (2006).

[31] Sahiner, B., Chan, H.-P., Petrick, N., Wei, D., Helvie, M. A., Adler, D. D., and Goodsitt, M. M., "Classification of mass and normal breast tissue: a convolution neural network classifier with spatial domain and texture images," *IEEE transactions on Medical Imaging* **15**(5), 598–610 (1996).

[32] Dominguez, A. R. and Nandi, A. K., "Detection of masses in mammograms via statistically based enhancement, multilevel-thresholding segmentation, and region selection," *Computerized Medical Imaging and Graphics* **32**(4), 304–315 (2008).

[33] Kashyap, K. L., Bajpai, M. K., and Khanna, P., "An efficient algorithm for mass detection and shape analysis of different masses present in digital mammograms," *Multimedia Tools and Applications* **77**(8), 9249–9269 (2018).

[34] Mambou, S. J., Maresova, P., Krejcar, O., Selamat, A., and Kuca, K., "Breast cancer detection using infrared thermal imaging and a deep learning model," *Sensors* **18**(9), 2799 (2018).

[35] Agaian, S. S., Panetta, K., and Grigoryan, A. M., "Transform-based image enhancement algorithms with performance measure," *IEEE Transactions on Image Processing* **10**(3), 367–382 (2001).

[36] Agaian, S. S., Silver, B., and Panetta, K. A., "Transform coefficient histogram-based image enhancement algorithms using contrast entropy," *IEEE transactions on image processing* **16**(3), 741–758 (2007).

[37] Silva, E. A., Panetta, K., and Agaian, S. S., "Quantifying image similarity using measure of enhancement by entropy," in [*Mobile Multimedia/Image Processing for Military and Security Applications 2007*], **6579**, 65790U, International Society for Optics and Photonics (2007).

[38] Panetta, K. A., Wharton, E. J., and Agaian, S. S., "Human visual system-based image enhancement and logarithmic contrast measure," *IEEE Transactions on Systems, Man, and Cybernetics, Part B (Cybernetics)* **38**(1), 174–188 (2008).

[39] Silver, B., Agaian, S., and Panetta, K., "Contrast entropy based image enhancement and logarithmic transform coefficient histogram shifting," in [*Proceedings.(ICASSP'05). IEEE International Conference on Acoustics, Speech, and Signal Processing, 2005.*], **2**, ii–633, IEEE (2005).

[40] Nercessian, S. C., Panetta, K. A., and Agaian, S. S., "Non-linear direct multi-scale image enhancement based on the luminance and contrast masking characteristics of the human visual system," *IEEE Transactions on image processing* **22**(9), 3549–3561 (2013).

[41] Gao, C., Panetta, K., and Agaian, S., "A new color contrast enhancement algorithm for robotic applications," in [*2012 IEEE International Conference on Technologies for Practical Robot Applications (TePRA)*], 42–47, IEEE (2012).

[42] Grigoryan, A. M. and Agaian, S. S., "Image processing contrast enhancement," *Wiley Encyclopedia of Electrical and Electronics Engineering* , 1–22 (1999).

[43] Erat, O., Panetta, K., and Agaian, S., "Contrast enhancement for underwater images in maritime border protection," in [*2017 IEEE International Symposium on Technologies for Homeland Security (HST)*], 1–5, IEEE (2017).

[44] Qiao, Y., Wei, Z., and Zhao, Y., "Thermal infrared pedestrian image segmentation using level set method," *Sensors* **17**(8), 1811 (2017).

[45] Silva, L., Saade, D., Sequeiros, G., Silva, A., Paiva, A., Bravo, R., and Conci, A., "A new database for breast research with infrared image," *Journal of Medical Imaging and Health Informatics* **4**(1), 92–100 (2014).

[46] EtehadTavakol, M., Sadri, S., and Ng, E., "Application of k-and fuzzy c-means for color segmentation of thermal infrared breast images," *Journal of medical systems* **34**(1), 35–42 (2010).

[47] Wang, X.-F., Huang, D.-S., and Xu, H., "An efficient local chan–vese model for image segmentation," *Pattern Recognition* **43**(3), 603–618 (2010).

[48] Liu, J. and Zhang, H., "Image segmentation using a local gmm in a variational framework," *Journal of mathematical imaging and vision* **46**(2), 161–176 (2013).

[49] Bhowmik, M. K., Gogoi, U. R., Majumdar, G., Bhattacharjee, D., Datta, D., and Ghosh, A. K., "Designing of ground-truth-annotated dbt-tu-ju breast thermogram database toward early abnormality prediction," *IEEE journal of biomedical and health informatics* **22**(4), 1238–1249 (2017).

[50] Powers, D. M., "Evaluation: from precision, recall and f-measure to roc, informedness, markedness and correlation," (2011).

[51] Dice, L. R., "Measures of the amount of ecologic association between species," *Ecology* **26**(3), 297–302 (1945).